ELSEVIER

Scopus

doi

Journal of Vibration Engineering

ISSN:1004-4523

Registered

- SCOPUS
- GOOGLE SCHOLAR
- DIGITAL OBJECT IDENTIFIER (DOI)
- IMPACT FACTOR 6.1

Our Website
www.jove.science

FINITE ELEMENT ANALYSIS OF THINNING, RESIDUAL STRESS, AND SPRINGBACK IN DEEP-DRAWN SQUARE CUPS

Duc Quang Vu
University of Economics – Technology for Industries
456 Minh Khai, Vinh Tuy Ward, Hanoi, Vietnam, 100000

Abstract:

This study employs a combined solution approach-Explicit for DD (DD) and Static/General for springback recovery-within finite element simulations to form six square cups from SUS304 stainless steel sheets using Abaqus/CAE. The research simultaneously addresses three critical issues: material thinning, residual stress, and springback along the forming depth. Thinning was analyzed through Abaqus/Explicit, while die release, residual stress, and springback were evaluated using Abaqus/Static/General to ensure accuracy in elastic recovery. Results at forming depths of H_{OZ} = 40÷75 mm indicate that maximum thinning occurs at the cup corners and increases with depth; residual stress is unevenly distributed, with tensile stress concentrated at corners, compressive stress at the bottom, and mixed stress along walls and rims; springback alters cup geometry after die release. Greater forming depths intensify plastic deformation, particularly at square corners due to biaxial stretching and friction. A safe forming threshold ($H_{OZ} \leq 55$ mm) was identified, where thinning remains below 20% of sheet thickness and residual stress and springback are within acceptable tolerances. The findings provide a quantitative dataset for predicting crack initiation and geometric deviation, offering practical guidance in selecting forming depth and optimizing die design or intermediate drawing steps. This work is directly applicable to the manufacturing of SUS304 square cup/box components in kitchenware, electronic casings, and automotive parts requiring high strength and corrosion resistance.

Keywords: *Deep drawing, SUS304 stainless steel, formability analysis, thinning, springback, residual stress, finite element simulation.*

1. INTRODUCTION

Deep drawing (DD) is a key sheet metal forming process widely applied in automotive, aerospace, packaging, and household appliance industries [1], [2]. It enables the production of complex geometries with high dimensional accuracy, mechanical strength, and minimal waste [2], [3]. However, the process faces challenges such as high tooling costs, long die manufacturing times, the need for high-capacity presses, and difficulties in controlling defects including wrinkling, tearing, and excessive thinning [1], [4]. Residual stress after forming and springback upon die release further complicate dimensional control and product quality [4]. Moreover, the process requires strict regulation of parameters such as blank-holder force, die radius, drawing speed, and lubrication [5], [6].

The Finite Element Method (FEM) has become indispensable in DD research, replacing costly experiments with numerical simulations that reduce development time and tooling costs [4], [7]. FEM allows prediction of stress and strain distributions, identification of failure-prone regions, evaluation of thinning, and optimization of die geometry. It also enables determination of optimal process parameters without extensive production trials [8]. Numerous studies have successfully applied FEM to analyze springback, thickness distribution, and thinning under varying die designs [7], [9].

Recent literature highlights extensive work on SUS304 stainless steel square cups. Yang and Chan used DEFORM-3D to simulate multi-step DD of electronic lock housings, analyzing blank-holder force effects on plastic flow and damage [10]. Another study employed FE simulation to establish forming conditions for SUS304 square cups free of delayed cracking, identifying a local thickening threshold below 47% at corners [11]. A combined DYNAFORM simulation and experimental study optimized one-step DD of SUS304 thin sheets, revealing anisotropic plasticity [12]. Obaeed examined AISI 1008 steel square cups, showing maximum thinning along walls did not exceed 25% of initial thickness [13]. Comparative work between hydromechanical DD (HMDD) and DD demonstrated HMDD achieved more uniform stress distribution, better thinning control, and reduced springback by up to 2.5 times [14]. A recent study on stainless steel 304 sink forming identified optimal parameters (corner radius R = 5 mm, drawing speed 20 mm/s, blank-holder force 3 MPa, friction coefficient 0.120), emphasizing the need to optimize one-step processes to eliminate intermediate annealing [12].

Despite these advances, several research gaps remain. Most studies focus on one or two quality indicators, lacking simultaneous evaluation of thinning, residual stress, and springback. No systematic comparison has been made of the influence of multiple forming depths on all three indicators in SUS304 square cups. The combined use of Abaqus/Explicit for thinning analysis and Abaqus/Static/General for residual stress and springback evaluation within a unified square cup model has not been comprehensively implemented. Furthermore, quantitative data on the variation of these indicators with forming depth, particularly in transition regions beyond safe limits, are scarce.

To address these gaps, this paper presents a finite element investigation of three key criteria-material thinning, residual stress, and springback-across six DD processes simulated in Abaqus/CAE [15], [16], [17]. Comparisons are made for square cups H40, H45, H50, H55, H65, and H75, corresponding to forming depths H_{OZ} = 40 mm, 45 mm, 50 mm, 55 mm, 65 mm, and 75 mm. Thinning is analyzed using Abaqus/Explicit throughout the drawing process, while residual stress and springback along OX, OY, and OZ axes are evaluated after die release using Abaqus/Static/General.

The findings provide valuable insights for the design and optimization of DD processes for SUS304 square cup/box components in kitchenware (sinks, pots, trays), electronic housings, and precision mechanical parts requiring high strength and corrosion resistance. They may also serve as references for sheet materials with mechanical properties similar to SUS304, such as stainless steels 201 and 316L, or high-strength DP steels.

2. Materials and Methods

2. 1. Die, punch, blank holder and blank models

Six DD processes were conducted to form six square cup specimens, designated H40, H45, H50, H55, H65, and H75. A quarter-symmetry geometric model of the die, punch, blank holder, and blank sheet was employed for finite element simulation, as illustrated in Figure 1. The punch had a side length of a_p = 100 mm, height h_p = 70 mm, with edges and punch head filleted at radius R_f = 10 mm. The die cavity had a side length of a_d = 102.5 mm, height h_d = 78.75 mm, and transition corners filleted with the same radius R_f = 10 mm. The blank was a square sheet with side length a_b = 200 mm and thickness t_b = 1.0 mm. The blank holder was designed to match the die, punch, and blank, with a clearance of 1.25 mm between die and punch. The blank material was SUS304 stainless steel, whose mechanical properties are listed in Table 1, and were used to define the plastic deformation material model in the finite element simulation. Mesh generation and boundary conditions for the punch, die, blank holder, and blank sheet were configured as summarized in Table 2.

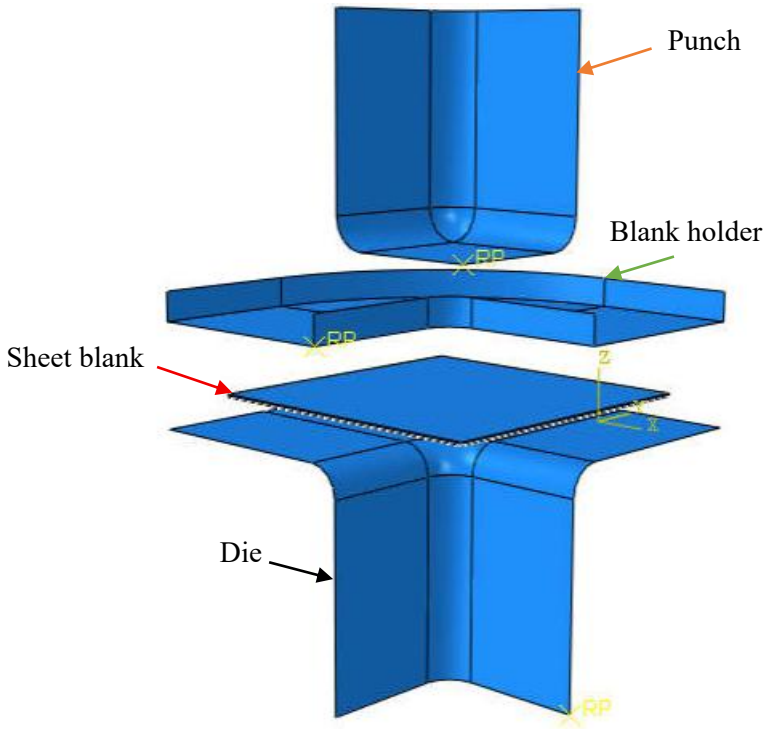

Figure 1. Geometric model of die, punch, blank holder, and blank used in six DD processes for specimens H40, H45, H50, H55, H65, and H75

Table 1. Material Properties of the SUS304 Sheet Blank

Material properties	**Value**
Temperature (^{o}C)	24
Density, ρ (kg/m^{3})	7850
Young's modulus, *E* (Gpa)	193
Hardening coefficient, *K* (MPa)	1275
Work hardening exponent, *n*	0.45
Poisson's ratio, ν	0.29
Yield strength, σ_Y (MPa)	226.3
Ultimate tensile strength, σ_U (MPa)	566.0
Elongation (%)	50.0

2. 2. Finite Element Simulation Setup

Finite element simulations for all six DD processes-H40, H45, H50, H55, H65, and H75-were performed in Abaqus/CAE using the quarter-symmetry die–punch–blank holder–blank model (Figure 1). The simulation type was Dynamic, Explicit, as specified in Table 2. Boundary conditions included a friction coefficient of 0.125 between blank and die, while contact between blank and blank holder was modeled using Abaqus/Explicit default "hard" normal contact, with no friction and no thermal interaction. Punch displacement was applied following the Amp-1 (Smooth Step) loading curve, and a concentrated blank-holder force of 22,870 N was imposed.

Table 2. Finite element simulation setup for the forming processes

Name	**Modeling**	**Type**	**Basic**	**Mesh (1/4 model) and**

	Space		Feature (Shap)	Boundary Condition
Forming (Dynamic, Explicit)				
SUS304Sheetblank	3D	Deformable	Shell	2500 elements, type = S4D - Explicit
Punch	3D	Discrete rigid	Shell	328 elements, type = R3D4 - Explicit. - OZ axis displacement: H_{OZ} = 40; 45; 50; 55; 65; 75 mm.
Die	3D	Discrete rigid	Shell	432 elements, type = R3D4 - Explicit. - Fixed.
Blankholder	3D	Discrete rigid	Shell	144 elements, type = R3D4 - Explicit. - Fixed.
Springback (Static, General)				
SUS304Sheetblank	3D	Deformable	Shell	2500 elements, type = S4D - Explicit.

After completion of each of the six DD processes, the punch, die, and blank holder were removed, leaving the geometric and mesh models of the six square cups (H40÷H75). Figure 2 shows the geometry and mesh of the square cup formed at H_{OZ} = 50 mm. For springback analysis, finite element simulations were conducted using the Static, General procedure in Abaqus, as summarized in Table 2.

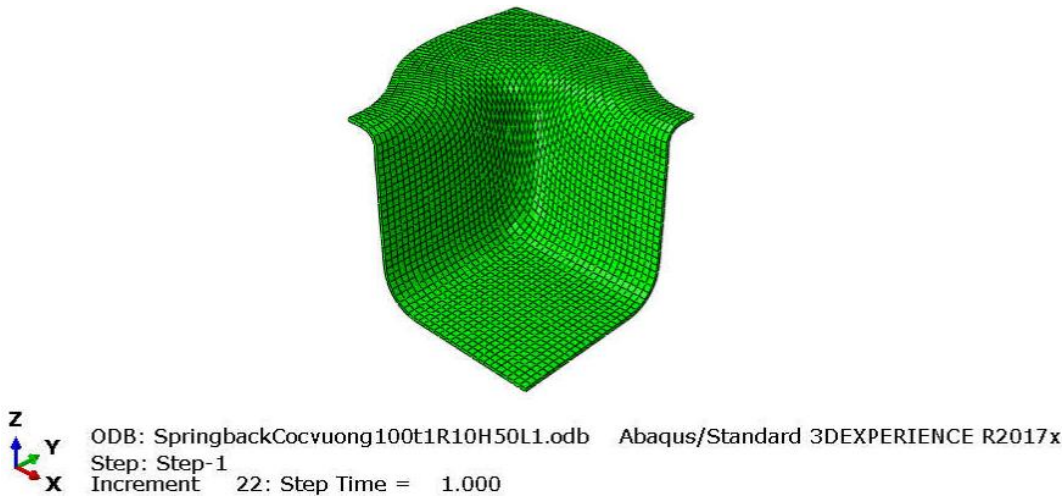

Figure 2. Geometry and mesh model of specimen H50

3. Results and Discussion

3.1. Material Thickness Distribution

The distribution of sheet thickness (STH) in the six specimens H40, H45, H50, H55, H65, and H75 is one of the most critical indicators reflecting their forming quality. The STH distributions of H40 and H75 are illustrated in Figures 3a and 3b. Both specimens exhibit the most severe thinning concentrated at the four rounded corners of the cup wall, where the material is subjected to a triaxial tensile stress state. For H40, the minimum thickness is $STH_{min\text{-}H40}$ = 0.85 mm, corresponding to a thinning ratio of $\varepsilon_{min\text{-}H40}$

= -15%, which remains within the safe limit [ε_{min}] = -30%. For H75, the minimum thickness is $STH_{min-H75}$ = 0.79 mm, corresponding to $\varepsilon_{min-H75}$ = -21%, also within the safe limit. In the deeper specimen H75, the flat wall region closer to the cup bottom experiences stronger thinning ($STH_{min-H75}$ = 0.79 mm), while the upper wall region near the rim undergoes significant thickening ($STH_{max-H75}$ = 1.41 mm, equivalent to $\varepsilon_{max-H75}$ = 41%). In contrast, the shallower specimen H40 shows only mild thinning near the bottom ($STH_{min-H40}$ = 0.85 mm), and the upper wall thickness remains nearly unchanged compared to the initial blank. This difference arises from variations in material flow along the forming depth, despite the wall being subjected to a plane stress–strain condition.

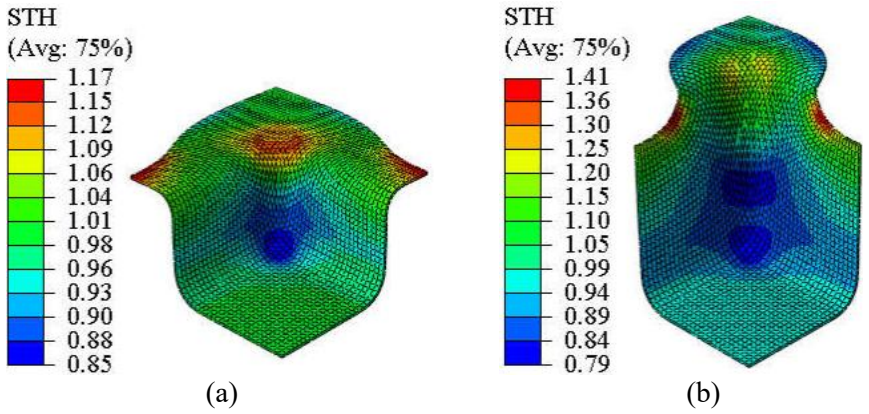

Figure 3. Distribution of sheet thickness (STH) in two specimens: (a) H40, (b) H75

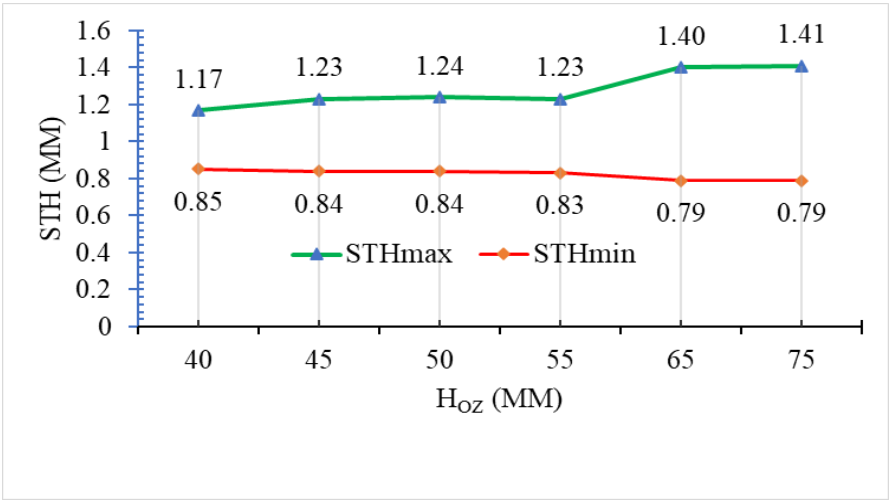

Figure 4. Comparison chart of minimum and maximum sheet thickness (STH_{min} and STH_{max}) across six specimens H40, H45, H50, H55, H65, and H75

Figure 4 compares the minimum and maximum wall thicknesses across all six specimens. As forming depth increases, both thinning and thickening intensify. The four corner regions consistently exhibit the strongest thinning, yet remain within the safe limit of [ε_{min}] = -30%. For forming depths H_{OZ} = 40÷55 mm, thinning is relatively uniform with STH_{min} = 0.83 ÷ 0.85 mm. At greater depths (H_{OZ} = 65÷75 mm), thinning reaches STH_{min} = 0.79 mm. Regarding thickening, specimens with H_{OZ} = 40÷55 mm show maximum thickening at the rim, concentrated in four small regions at the midpoints of each rim edge, with STH_{max} = 1.17 ÷ 1.24 mm. For deeper specimens (H_{OZ} = 65÷75 mm), maximum thickening occurs along the wall in eight localized transition zones between the cup ears and the wall, reaching STH_{max} = 1.40 ÷ 1.41 mm.

3.2. Residual Stress

The distribution of residual stress (S) in two square cup specimens with forming depths H_{OZ} = 40 mm and H_{OZ} = 75 mm, after removal of the punch load and die release, is shown in Figures 5a and 5b. The stress distribution patterns in both specimens are relatively similar. The maximum residual stress is concentrated in four small regions located at the midpoints of the cup wall, near the transition radius between the wall and the rim. For H40, the maximum residual stress is $S_{max\text{-}H40}$ = 410.58 MPa, which is below the ultimate tensile strength σ_U = 566.00 MPa. For H75, the maximum residual stress reaches $S_{max\text{-}H75}$ = 566.00 MPa, equal to σ_U. The minimum residual stress is primarily distributed at the cup bottom, with values of $S_{min\text{-}H40}$ = 10.17 MPa and $S_{min\text{-}H75}$ = 9.37 MPa, both much lower than σ_Y = 226.3 MPa.

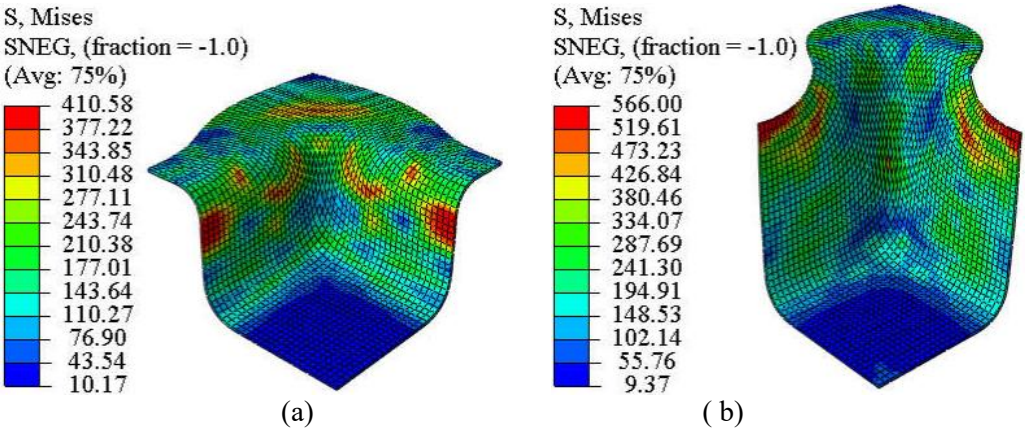

Figure 5. Distribution of residual stress (S) in two specimens: (a) H40, (b) H75

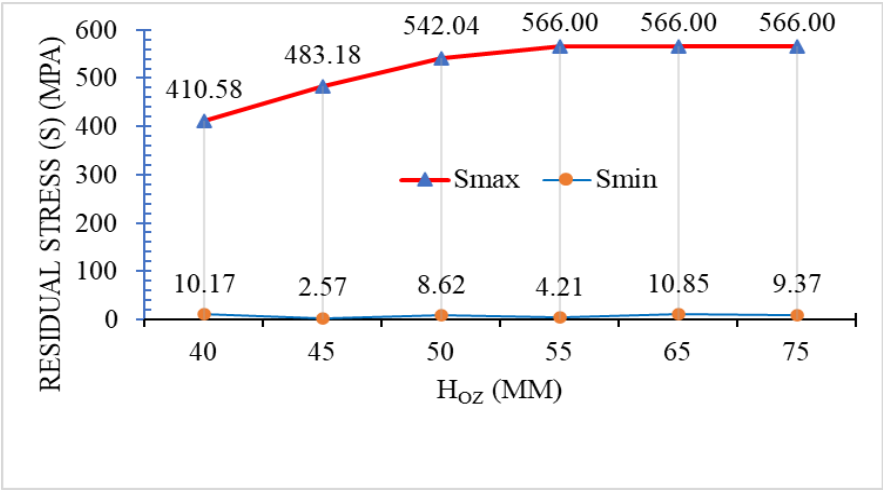

Figure 6. Comparison chart of minimum and maximum residual stress (S_{min} and S_{max}) across six specimens H40, H45, H50, H55, H65, and H75

Figure 6 compares the minimum and maximum residual stresses across all six specimens (H40÷H75). A consistent trend is observed: as forming depth increases, S_{max} rises until it reaches the ultimate tensile strength σ_U = 566.00 MPa. Meanwhile, the minimum residual stress remains very low, in the range S_{min} = 2.57 ÷ 10.85 MPa, far below the yield strength σ_Y = 226.3 MPa. For forming depths H_{OZ} = 40 ÷ 55 mm, S_{max} increases sharply from 410.58 MPa to 566.00 MPa. In contrast, for H_{OZ} = 55÷75 mm, S_{max} remains constant at 566.00 MPa, indicating that the material undergoes stronger strain hardening at greater depths. To stabilize the geometry and mitigate fatigue behavior of the

formed components, residual stress relief treatments-such as thermal or mechanical methods-may be applied.

3. 3. Springback

Springback along the three axes OX (U1), OY (U2), and OZ (U3) in specimens H40 and H75, after removal of the punch load and die release, is illustrated in Figures 7a and 7b. In specimen H40, the maximum springback along OX and OY is similar, with $U1_{max\text{-}H40}$ = 0.28 mm (represented by red vectors) and $U2_{max\text{-}H40}$ = 0.29 mm (represented by blue vectors), both directed inward toward the cup cavity. In contrast, specimen H75 shows slightly different values, with $U1_{max\text{-}H75}$ = 0.75 mm and $U2_{max\text{-}H75}$ = 0.67 mm, both directed outward from the cup cavity. The maximum springback along OZ occurs at the tips of the four cup ears, farthest from the cup center, with $U3_{max\text{-}H40}$ = 1.24 mm and $U3_{max\text{-}H75}$ = 0.89 mm, both oriented downward.

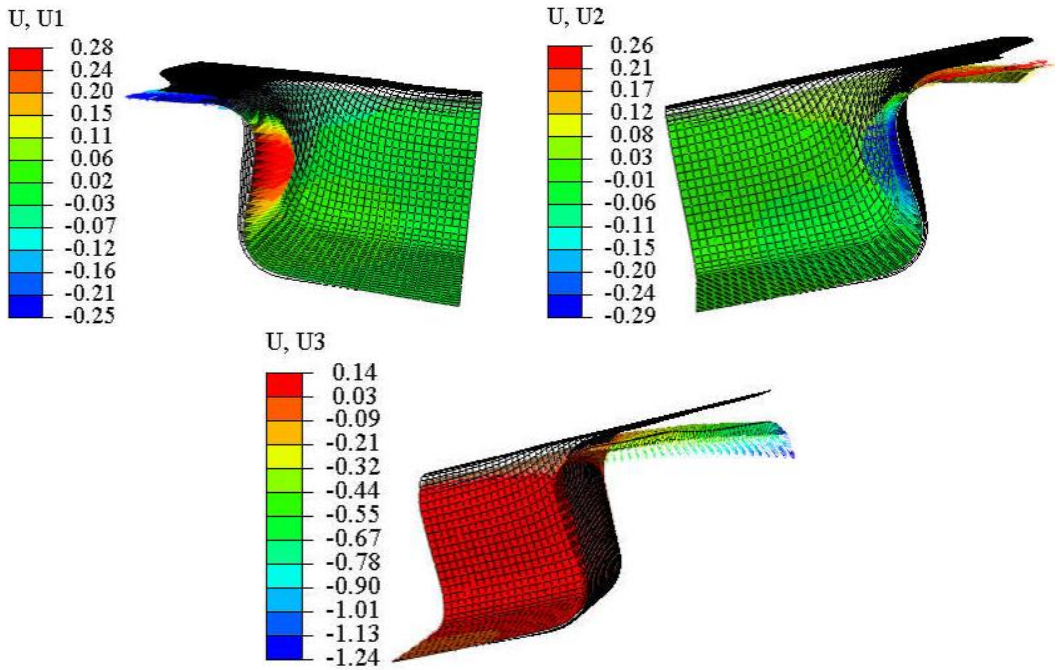

a)

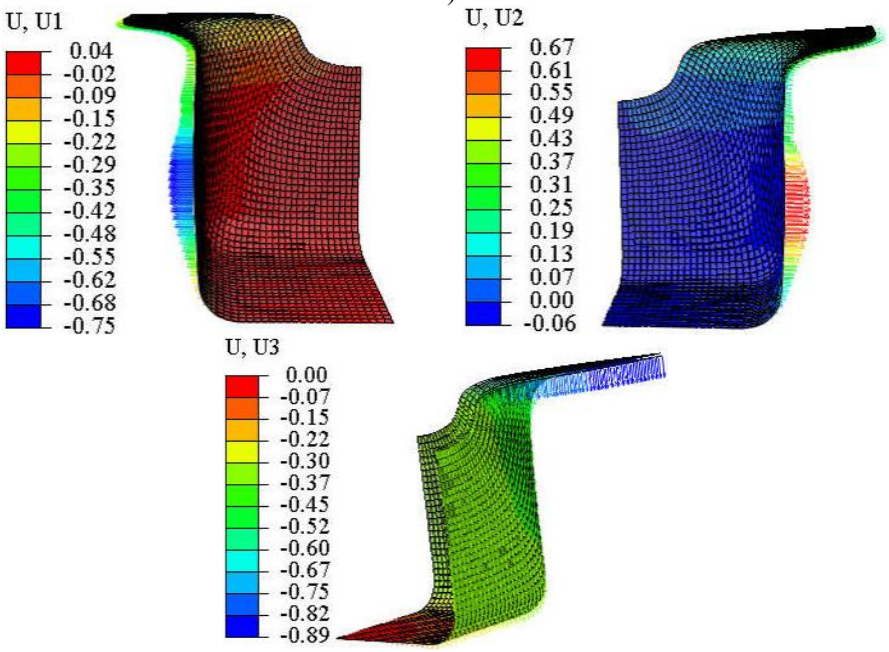

b)

Figure 7. Distribution of springback displacements U1, U2, and U3 in two specimens: (a) H40, (b) H75

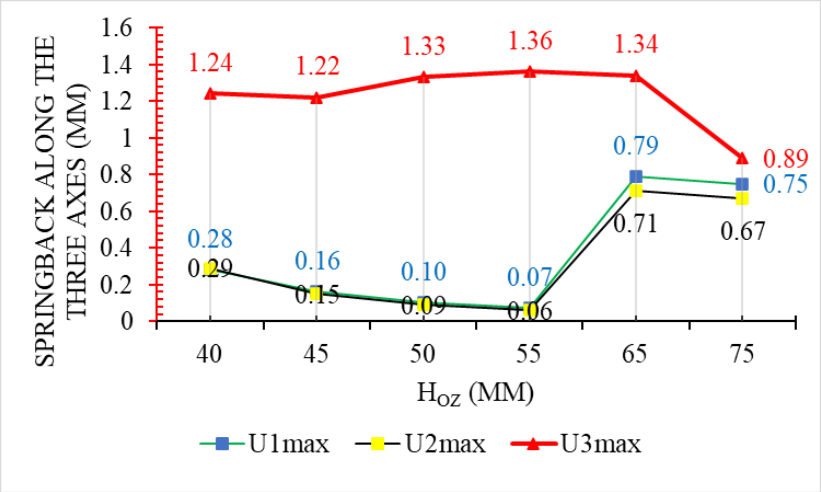

Figure 8. Comparison chart of maximum springback displacements ($U1_{max}$, $U2_{max}$, $U3_{max}$) across six specimens H40, H45, H50, H55, H65, and H75

Figure 8 compares the maximum springback values $U1_{max}$, $U2_{max}$, $U3_{max}$ across all six specimens (H40÷H75). The results show that $U1_{max} \approx U2_{max}$ for each forming depth. Their values decrease from 0.29 mm to 0.06 mm as forming depth increases from H_{OZ} = 40 mm to H_{OZ} = 55 mm, but then rise sharply from 0.06 mm to 0.79 mm as depth increases further to H_{OZ} = 75 mm. Springback along OZ remains relatively stable in the range 1.24÷1.36 mm for H_{OZ} = 40÷65 mm, but decreases significantly from 1.34 mm to 0.89 mm when depth increases from H_{OZ} = 65 mm to H_{OZ} = 75 mm. A noteworthy observation is that at H_{OZ} = 75 mm, the maximum springback values along all three axes become comparable, with $U1_{max}$ = 0.75 mm ≈ $U2_{max}$ = 0.67 mm ≈ $U3_{max}$ = 0.89 mm. This indicates a convergence of springback behavior at greater forming depths.

3.4. Limitations and future research directions

Although this study provides valuable numerical simulation results regarding thinning, residual stress, and springback of SUS304 square cups at six different forming depths, several limitations remain that must be addressed to ensure reproducibility and practical applicability. First, the investigation was limited to a single material (SUS304 stainless steel), one sheet thickness, and a fixed set of process parameters (blank-holder force, friction coefficient, punch/die corner radius, and die clearance). The findings are therefore confined to these specific conditions. Any variation-for example, increasing blank-holder force to reduce wrinkling but simultaneously intensifying thinning, or altering corner radius which directly affects stress distribution-could significantly change the trends and magnitudes of thinning, residual stress, and springback. Second, the study was conducted entirely through numerical simulations in Abaqus/CAE without experimental validation. While the finite element models were based on widely accepted plasticity and elasticity theories, discrepancies between simulation and reality inevitably exist due to idealized assumptions. Third, the forming depth range was restricted to 75 mm. Results revealed nonlinear behavior beyond 55 mm, yet the actual failure depth limit was not determined. Moreover, the square cup geometry investigated had fixed side length and corner radius, limiting generalization. Fourth, other influential process parameters such as drawing speed, multi-step forming, temperature, and lubrication

conditions were not considered. These factors play critical roles in industrial practice, particularly for SUS304, which exhibits high work-hardening and friction sensitivity.

Based on these limitations, future research should pursue several directions: Experimental validation of SUS304 square cup forming at H_{OZ} = 40÷75 mm, including measurements of thinning, springback, and residual stress, to calibrate and enhance the reliability of FEM models. Multi-parameter investigations examining the combined effects of forming depth, blank-holder force, punch/die corner radius, friction coefficient, and drawing speed on the three quality indicators. Advanced constitutive modeling, incorporating anisotropy, the Bauschinger effect, and strain-rate sensitivity, to more accurately capture complex deformation, especially at cup corners. Process innovations such as multi-step forming with intermediate annealing or hydromechanical DD, to improve strain distribution, reduce localized thinning, and control springback in deep cups exceeding 55 mm. Predictive modeling frameworks integrating simulation and experimental data, enabling rapid estimation of thinning, residual stress, and springback across varying depths and process parameters without repeated FEM runs. Extension to other geometries and materials, including round cups, rectangular cups with different aspect ratios, and alternative sheet metals such as stainless steels 201 and 316L, DP600 steel, and aluminum 6061, to build a comprehensive comparative dataset and derive generalized rules on the influence of forming depth on DD quality.

4. Conclusions

This study conducted numerical simulations of six DD processes to form six square cups (H40, H45, H50, H55, H65, and H75) from SUS304 stainless steel sheets using Abaqus/CAE. A combined approach was applied: Abaqus/Explicit for analyzing material thinning during forming, and Abaqus/Static/General for evaluating residual stress and springback after die release. Six forming depths (H_{OZ} = 40 mm, 45 mm, 50 mm, 55 mm, 65 mm, and 75 mm) were investigated to compare their influence on three critical quality indicators. The main conclusions are as follows:

1. Material Thinning: Maximum thinning occurs at the four corners of the square cups, where biaxial tension and high friction are concentrated. Thinning increases with forming depth. At H_{OZ} = 40 mm, the maximum thinning ratio is $\varepsilon_{min\text{-}H40}$ = -15%;; at H_{OZ} = 75 mm, it reaches $\varepsilon_{min\text{-}H75}$ = -21%;, approaching the critical limit [ε_{min}] = -30%, indicating risk of tearing. This trend confirms forming depth as a key parameter controlling thickness reduction, with a safe one-step forming threshold recommended at $H_{OZ} \leq$ 55 mm to maintain thinning below 20%.

2. Residual Stress: After die release, residual stress is unevenly distributed. Significant tensile residual stress appears in the wall and corner regions, while compressive residual stress is concentrated at the cup bottom. Residual stress increases with forming depth, showing a sharp transition beyond H_{OZ} = 55 mm, where $S_{max\text{-}H55}$ = 566.00 MPa = σ_U = 566.00 MPa. This indicates that beyond this depth, SUS304 accumulates elastic residual stress rather than fully releasing it through plastic deformation, negatively impacting fatigue resistance and corrosion performance.

3. Springback: Springback was evaluated through displacements along three axes (U1, U2, U3). The largest displacement occurs along OZ, highly sensitive to forming depth, increasing from $U3_{max\text{-}H45}$ = 1.24 mm to $U3_{max\text{-}H65}$ = 1.34 mm. Displacements along OX and OY are smaller but rise significantly at H_{OZ} = 75 mm, causing dimensional deviations beyond tolerance in precision applications. Greater forming depths intensify springback due to accumulated residual stress and the high elastic modulus of SUS304.

Overall, all three indicators-thinning, residual stress, and springback-exhibit nonlinear trends with forming depth. H_{OZ} = 55 mm is identified as a critical transition point: from 40 to 50 mm, values increase linearly and remain within acceptable limits; beyond 55 mm, all indicators rise sharply, marking an unsafe zone for one-step DD without auxiliary measures. This study provides a quantitative dataset and transformation rules that serve as valuable references for engineers in designing and optimizing DD processes for SUS304 square cups.

Acknowledgments

This research was conducted with support from the University of Economics and Technology for Industries (https://uneti.edu.vn/), Vietnam.

References

[1] *C. Jai Shiva Rao, K. Prasanna Lakshmi, M.Venkata Ramana, Jalumedi Babu, "Advanced deep drawing methods, challenges, and future scope - A Review", Mechanical Engineering for Society and Industry, vol. 4, no. 3,* ***(2024)****, pp. 490-512.*

[2] *Zainul Huda, "Metal Forming Processes: Fundamentals, Analysis, Calculations", Springer Cham,* ***(2024)****.*

[3] *The-Thanh L, Tien-Long B, The-Van T, Duc-Toan N, "A study on a deep-drawing process with two shaping states for a fuel-filter cup using combined simulation and experiment", Advances in Mechanical Engineering, vol. 11, no. 8,* ***(2019)****.*

[4] *C.V. Nielsen and P. A.F. Martins, "Metal Forming: Formability, Simulation, and Tool Design", 1st ed. London, England: Academic Press - Elsevier Inc,* ***(2021)****.*

[5] *Atul S T, Babu MCL, "A review on effect of thinning, wrinkling and spring-back on DD process", Proceedings of the Institution of Mechanical Engineers, Part B: Journal of Engineering Manufacture, 2019;vol. 233, no. 4,* ***(2019)****, pp. 1011-1036.*

[6] *Schuler GmbH, "Metal Forming Handbook", 1st ed, Springer, Berlin, Germany,* ***(1998)****.*

[7] *H. Zein, M. El Sherbiny, M. Abd-Rabou, M. El shazly, "Thinning and spring back prediction of sheet metal in the deep drawing procesa", Materials & Design, vol. 53,* ***(2014)****, pp. 797-808.*

[8] *Reimund Neugebauer, "Hydo-umformung", Springer Berlin, Heidelberg,* ***(2007)****.*

[9] *Koç, M., "Hydroforming for advanced manufacturing", 1st edn, Cambridge, England: Woodhead Publishing Limited and CRC Press LLC,* ***(2008)****.*

[10] *T. S. Yang and M. J. Chan, "Application of multi-pass stamping process of SUS304 stainless steel", Journal of Physics: Conference Series 3144* ***(2025)*** *012011, pp. 1-8.*

[11] *K. L. Ong and C. J. Tan, "Estimating Forming Conditions for Deep Drawn SUS304 Square Cups Having no Delayed Cracks Using FE Simulation", MSF, vol. 1078,* ***(2022)****, pp. 17-22.*

[12] *Li, Y., Xu, J., & Luan, B., "Investigation on Strain-Forming Limits and Manufacturing Optimization of a Single Deep-Drawing Process Concerning 304 Stainless Steel's Thin Sheet", Metals, vol. 15, no. 9,* ***(2025)****, 1008.*

[13] *Nareen H. Obaeed, "Numerical and Experimental Explorations for the Formability of Drawing Square Cups Through Deep Drawing Operation", Engineering and Technology Journal, vol. 38, no. 9A,* ***(2020)****, pp. 1316-1326.*

[14] *Duc, Quang. "A Comparative Simulation Study on Springback and Formability Square Cups: Hydromechanical vs. Conditional Deep Drawing", Journal of Machine Engineering, vol. 26, no. 1,* ***(2026)****, pp. 114-126.*

[15] *Abaqus/CAE 3DEXPERIENCE R2017X, Dassault Systemes SIMULIA Corp. 1301 Atwood Avenue, Suite 101W Jonhston, RI 02919, USA.*

[16] *Gong Y., Lou J., Hou W., Su L., Wang S., Dong L., "Cold Stamping Forming Simulation and Springback Analysis of High Strength Steel Plate for Automobile Body", Forest Chemicals Review,* ***(2022)****, pp. 1177-1187.*

[17] *Quang V.D., "The Optimization of Rotary Bending Die Process: Criteria for the Metal Sheet Angles and Springback Effects", Eng. Technol. Appl. Sci. Res., vol. 15, no. 1,* ***(2025)****, pp. 20553-20558.*